ISBN: 978-3-95450-211-0 doi:10.18429/JACoW-SRF2019-TUP054

HOW IS FLUX EXPULSION AFFECTED BY GEOMETRY: EXPERIMENTAL EVIDENCE AND MODEL

David Longuevergne
IPNO, CNRS-IN2P3, Université Paris Sud, Université Paris-Saclay, Orsay, France

Abstract

Measurements of magnetic sensitivity to trapped flux on several type of cavity geometries have been performed at IPNO showing a clear geometrical effect. Magnetic sensitivity depends not only on material quality but also on the cavity geometry and on the residual magnetic field orientation. A presentation of experimental data will be done. These will be as well compared to the theoretical magnetic sensitivities calculated thanks to a simple Labview routine-paper.

INTRODUCTION

Performances of a superconducting accelerating cavity made of bulk Niobium are strongly affected by the presence of a residual magnetic field while transiting into its superconducting state. Trapped vortices interact strongly with the radiofrequency (RF) electromagnetic fields inducing additional dissipations in the helium bath [1]. These additional losses can be modelled by a resistance R_{mag} dependent on temperature and, as it will be shown, on the RF field amplitude and orientation.

The total surface resistance of a superconductor is the sum of a temperature dependent contribution called the BCS resistance (derived from BCS theory of superconductivity, See Eq (1)) and a contribution defined as the residual resistance (remaining resistance at 0K, See Eq. (2)). This contribution is mainly due to material imperfections (pollution, defects, grain boundaries…) and obviously magnetic flux trapping.

$$R_S = R_{BCS}(f,T) + R_{res}(f,T) \quad (1)$$

$$R_{res} = R_0 + R_{mag}(f,T) \quad (2)$$

To prevent Niobium from trapping magnetic flux coming from earth or magnetic parts at the vicinity of the cavity, magnetic shields are installed around the superconducting cavity. High permeability material as permalloy (μ-metal), Cryophi® or A4K are used to funnel the magnetic field and thus attenuating strongly the residual magnetic field inside it. Specifications on the attenuation factor required to ensure good performances of the cavity are given by the total resistance tolerable and thus by the budget allocated to the magnetic contribution.

Once the project has specified the maximum R_{mag} allowable, the total attenuation H_{res}/H_{earth} required for the magnetic shield is given by Eq. (3):

$$R_{mag} = \eta_{mag} \cdot S_{mag}(f,T) \cdot H_{res} \quad (3)$$

Where η_{mag} is the flux trapping efficiency coefficient, S_{mag} the magnetic sensitivity of the cavity expressed in nΩ/mG and H_{res} the mean residual magnetic field present at transition. A simple empirical model [1] gives a good approximation of S_{mag} as formulated in Eq. (4):

$$S_{mag} = \frac{R_n(f,T)}{2 \cdot H_{c2}(T)} \quad (4)$$

With R_n the normal resistance and H_{c2} the second critical field of the material.

As it will be discussed in this paper, the real magnetic sensitivity is extremely difficult to predict as this one can depend on many parameters:

- Frequency of the cavity. Sensitivity scales with the square root of frequency given by the frequency dependence of a resistive material subject to a RF field.
- Geometry of the cavity. The residual trapped flux is not the same depending on the orientation of the magnetic field versus the cavity walls [2].
- Quality of surface and material. The more pinning centers are present in the material, the more vortices can be trapped while transiting and reduce flux expulsion efficiency [3].
- Cooling-down conditions (thermal gradient, cooling speed, …). Thermal gradients promote field expulsion when material quality is good enough [4].

This paper will give details on magnetic sensitivity measurements of three types of cavities.

The first is a Quarter-Wave Resonator (QWR) made of bulk Niobium operating at a frequency of 88 MHz built for Spiral2 project [5]. The second is a Double-Spoke Resonator (DSR) made of bulk Niobium operating at 352 MHz for ESS project [6]. And the third is Simple-Spoke Resonator (SSR) made of the same material and operating at the same frequency for MYRRHA project [7].

EXPERIMENTAL SET-UP

The Vertical Cryostat

In an effort to fully qualify any new cavity design or a new surface treatment process or procedure, cavities are first tested in what is commonly called a “vertical cryostat”. Contrary to accelerating module used on an accelerator and optimized in that sense, vertical cryostats are optimized to provide optimal testing conditions to address cavity performances. The intrinsic quality factor (noted Q_0) is evaluated at different accelerating gradient (noted E_{acc}) by measuring the power dissipated in the cavity walls Pc. The cryostat available at IPNO (Institut de Physique Nucléaire d’Orsay) in operation since 1998 and upgraded in 2018 is capable of hosting two jacketed cavities (equipped with their helium jacket) in a volume constrained in a cylinder of 2 m high and 1.15 m in diameter.

The cryostat is externally shielded on the side by 1mm-thick permalloy sheets rolled around the vacuum vessel.

ISBN: 978-3-95450-211-0 doi:10.18429/JACoW-SRF2019-TUP054

The horizontal component of the magnetic field is significantly attenuated. Because of design constraints, the vertical component is not shielded by permalloy sheets installed on the top and bottom of the cryostat but by three compensating coils inserted in between the magnetic shield and the vacuum vessel as depicted in Figure 1. This configuration allows either to reduce the magnetic field to a minimum value to optimize the cavity performances or to apply a uniform vertical field to evaluate the magnetic sensitivity to vertical field of any cavity. Figure 2 shows two examples of magnetic configurations of residual field.

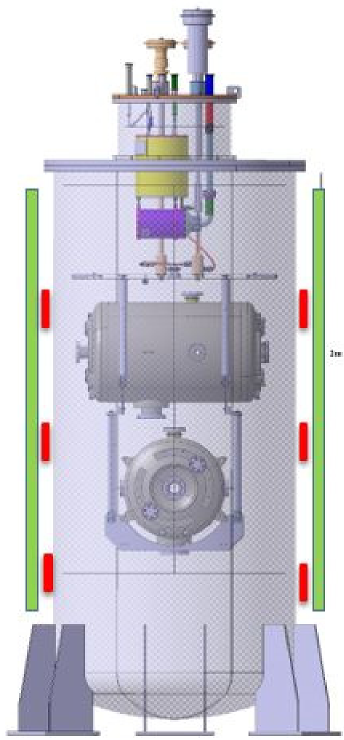

Figure 1: Vertical cryostat in operation at IPNO with its passive and active magnetic shields. The insert is loaded with two ESS Double Spoke Resonators.

Magnetic Sensors

Regarding magnetic measurement, the very low magnetic field to be measured makes the fluxgate magnetometer the best technology in our test conditions (vacuum, low temperatures). As fluxgate sensors adapted to cryogenic environment are only available as single axis sensors, three of them are assembled on a support to measure the three axis. A home-made multiplexer has been built to read up to twelve type G sensors with only one controller (MAG01-H) from Bartington [8]. The magnetic field resolution is of 0.02 mG over a range of 20 G. Integration time imposes a minimum multiplexing rate rather slow of about six seconds. To avoid any crosstalk between sensors, both current and voltage leads are multiplexed. Only one sensor is energized at a time.

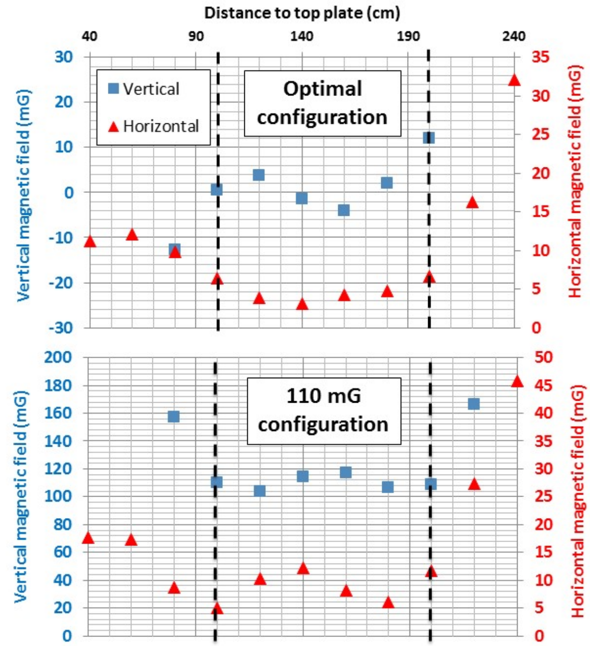

Figure 2: Example of residual magnetic field configuration applied in IPNO vertical cryostat. The vertical and horizontal components are measured along the central axis of the cryostat

Measurement Capabilities

Several types of measurements are possible with the current set-up:

- Evaluation of the magnetic sensitivity to residual vertical magnetic field of different type of superconducting cavities (S_{mag}).
- Evaluation of the flux trapping efficiency (η_{mag}). Usually complicated to achieve on cavities as they are equipped with a helium tank limiting significantly the cavity accessibility for instrumentation.
- Monitor magnetic field behaviour during cooling down generated by thermos-currents because of the existence of bi-metallic junctions.
- Evaluate magnetic shield efficiency.

This paper will only focus on sensitivity measurements of three different cavities as depicted in Figure 3. Vertical sensitivity has been measured on Spiral2 QWR and MYRRHA SSR whereas the longitudinal sensitivity of ESS DSR has been measured as this cavity has been installed vertically in the cryostat.

Cooling speed through transition has also been investigated on Spiral2 QWR and MYRRHA SSR without any measurable effect on the residual resistance even-though some differences have been observed on the flux expulsion [7,9].

The surface exposed to the intense radiofrequency electromagnetic field of these three cavities have been prepared following the standard procedure with SUPRATECH facilities at IPNO:

- Degreasing in an ultrasonic bath with detergent.
- Surface abrasion by Buffered Chemical Polishing of at least 200 µm (BCP)

ISBN: 978-3-95450-211-0 doi:10.18429/JACoW-SRF2019-TUP054

- Optional hydrogen degassing at 650°C during 10 h.
- High Pressure Rinsing with ultra-pure water
- Drying and assembly in ISO4 clean room

Based on experiments done on polycrystalline Niobium and at the sight of the surface preparation performed, we can consider η_{mag} as a constant and equal to 1. Indeed, without any recrystallization process, close to 100% of the residual magnetic field is trapped [10].

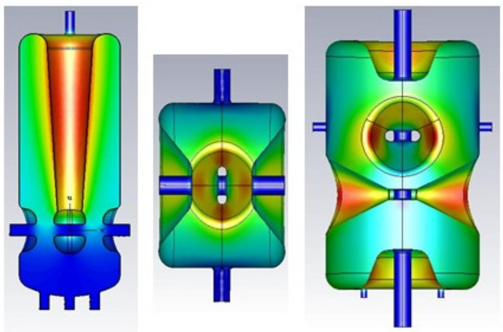

Figure 3: From left to right, RF magnetic field distribution of: Spiral2 QWR, MYRRHA Single Spoke Resonator (SSR) and ESS Double Spoke Resonator (DSR).

EXPERIMENTAL RESULTS

The magnetic sensitivity is estimated thanks to the following procedure:

- The cavity is cooled down in an ambient residual magnetic field as low as possible as depicted previously in Figure 2. The vertical component stays below 10 mG as well as the horizontal component
- The surface resistance at low field is estimated from the Q_0 measurement and with Eq. (5)

$$R_S = \frac{G}{Q_0} \quad (5)$$

- The cavity is warmed up slowly above transition during the night (>50 K) and then cooled down in a homogeneous vertical magnetic field up to 110 mG (See Figure 2). The horizontal component stays below 15 mG.
- The magnetic sensitivity is then derived from Eq. (3) by considering that the flux is fully trapped. We obtain the following formula Eq. (6):

$$S_{mag} = \frac{\Delta R_s}{\Delta H_{res}} \quad (6)$$

The sensitivities measured on the three types of cavities are summarized in Table 1.

Table 1: Measured Sensitivities (nΩ/mG)

Type of cavity	Measured component	Theoretical sensitivity*	Measured sensitivity (error)
QWR	Vertical	0.08	0.006 (-93%)
QWR	Horizontal	0.08	0.050 (-38%)
SSR	Vertical	0.12	0.043 (-64%)
DSR	Beam axis	0.12	0.060 (-50%)

*Estimated from Eq. (4).

Geometrical Dependence

One can appreciate from experimental data in Table 1 that the measured sensitivities are systematically and significantly lower than the theoretical sensitivities. Moreover, the difference of sensitivity of the QWR to a vertical or horizontal field (See Figure 4) is suggesting very strongly a geometrical dependence.

The fact that RF magnetic field are mainly distributed around the inner conductor, meaning around an almost vertical surface could explain these observations. Indeed, as the surface resistance is estimated from Q_0, or in other word from power dissipations, a change in surface resistance could be measured only if this occurs in RF magnetic field regions. Trapping flux on the bottom of the QWR, for example, wouldn't make the Q_0 drop as only RF magnetic fields (and not electric fields) are dissipating.

However, this fact only is not sufficient to cause this geometrical dependence. The flux trapping mechanism has to be as well dependent on the angle between the cavity surface and the residual magnetic field. In the literature, magnetization studies (reversible and irreversible) on type-II thin films have been performed and would confirm the angular dependence. For low magnetic fields (<< H_{c2}), the irreversible magnetization M_{irr}, meaning the remaining trapped vortices, tends to be equal to the normal component to the surface of the applied field $H_\perp$ and not to the norm of H_{res} [2]. These results would be in good agreement with our observations and hypothesis.

Field Dependence

During all flux trapping experiments and systematically for all three types of cavities, the same behaviour of the surface resistance versus the amplitude of the RF field has been observed. The field dependence of the surface resistance, and more specifically the linear dependence is strengthened with the amount of trapped flux as shown in Figure 4 and Figure 5.

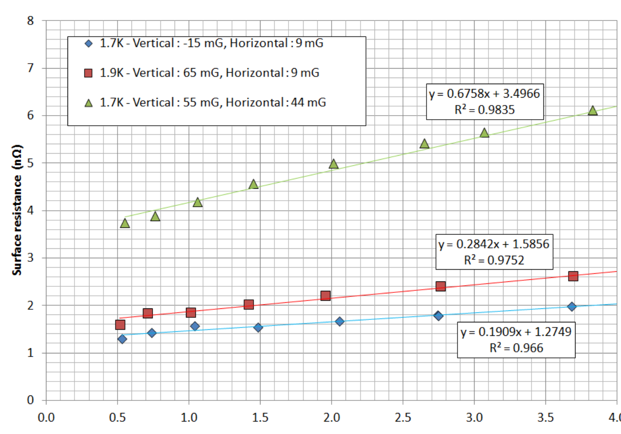

Figure 4: Surface resistance plotted versus accelerating gradient of a Spiral2 QWR for different ambient magnetic field applied: optimal (diamonds), vertical (square) and horizontal (triangle).

ISBN: 978-3-95450-211-0 doi:10.18429/JACoW-SRF2019-TUP054

The surface resistance R_s can be interpolated linearly at fields below 4 MV/m with the following Eq.(7):

$$R_s = R_0 + R_1 \cdot E_{acc} \quad (7)$$

With R_0 the zero-field surface resistance and R_1 the linear coefficient and E_{acc} the accelerating gradient.

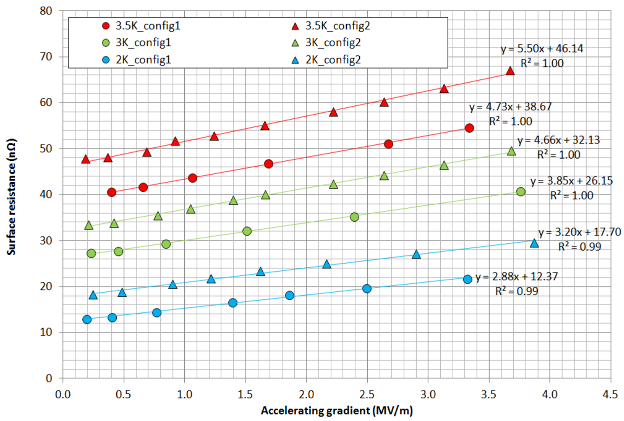

Figure 5: Surface resistance plotted versus accelerating gradient of a ESS DSR for two different ambient magnetic field applied: low (circle) and high (triangle) and at three different temperatures: 3.5K, 3K and 2K.

The last plot is highlighting a very interesting behaviour of the surface resistance versus accelerating field. The linear coefficient R_1 is increased not only by residual magnetic field but also by temperature. This tends to show that the linear dependence is not only caused by trapped flux but more generally by any contributions to the surface resistance (BCS, material defects, …). Figure 6 is summarizing the correlation between R_0 and R_1 for all three cavities at different trapped magnetic field level (encircled), temperatures and heat treatments.

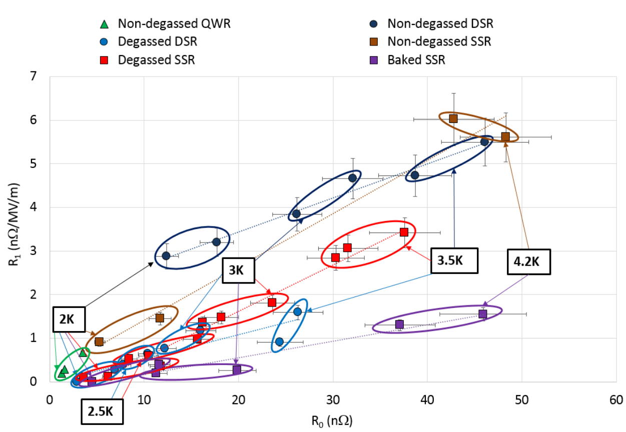

Figure 6: Linear coefficient (R_1) correlation with zero-field coefficient (R_0) for Spiral2 QWR (triangle), ESS DSR (circle) and MYRRHA SSR (square) between 4.2K and 2K and for different heat treatments (10h - 650°C hydrogen degassing and 48h - 120°C baking).

The strong impact of heat treatments on both coefficients suggests that the linear dependence

Any material property modification makes the correlation change significantly depending on the heat treatment done. Indeed, the hydrogen degassing treatment shifts the curves down without changing significantly the slope. Hydrogen degassing is known to prevent any precipitation of Niobium hydrides behaving like weak links. These weak links, as explained in [11], induce a linear increase of the surface resistance versus RF field. It makes then sense that hydrogen degassing shifts down R_1 as the contribution coming from Niobium hydride becomes zero. On the other hand, the 120°C baking seems to mitigate the dependence of R_1 versus R_0. Additional investigations are being performed to understand these strong correlations.

MODEL TO EXPLAIN GEOMETRICAL EFFECT

As stressed previously, the measured magnetic sensitivities are systematically lower than the theoretical model. Moreover, the relative error between the measured and theoretical sensitivities is changing with the type of cavity and the magnetic residual field orientation. This suggests that material properties of Niobium are not the only driving parameters but geometry as well.

Model Description

The model proposed here is based on one strong assumption as described earlier: only the normal component to the cavity surface of the ambient magnetic field can be trapped in the material. This hypothesis, observed experimentally in 1999 [2], as it will be shown, will lead to a very good agreement between measured and predicted sensitivities.

Moreover, as surface resistance is measured in SRF cavities indirectly and globally through power dissipations, the model has to:

- Evaluate the real trapped flux and calculate the additional resistance R_{mag} thanks to Eq. (8):

$$R_{mag} = R_n(f,T) \cdot \frac{H_\perp}{2 \cdot H_{c2}} \quad (8)$$

  With f the frequency of the cavity, σ_n, RRR and H_{c2} respectively the normal conductance, Resistance Residual Ratio and the second critical field of Niobium and $H_\perp$ the normal to surface component of the residual ambient magnetic field.
- Evaluate the additional local power dissipation. Trapped flux induces additional losses only in RF magnetic regions.
- Integrate the overall sensitivity S_{mag} all over the geometry with Eq. (9):

$$S_{mag} = \frac{\iint_S R_{mag} \cdot H_{RF}^2 \cdot dS}{H_{ext} \cdot \iint_S H_{RF}^2 \cdot dS} \quad (9)$$

  With H_{RF} the local RF magnetic field and H_{ext} the residual ambient magnetic field.

This model has been computed thanks to NI Labview software and requires exported files generated by CST Microwave Studio like surface magnetic field distribution and

ISBN: 978-3-95450-211-0 doi:10.18429/JACoW-SRF2019-TUP054

surface mesh [12]. Figure 7 depicts the three kind of graphical output generated by the code.

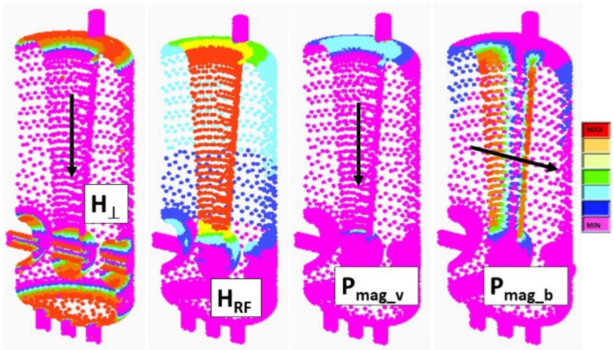

Figure 7: Outputs from Labview routine showing from left to right: the trapped magnetic field ($H_\perp$), the RF magnetic field distribution (H_{RF}), the normalized power dissipations caused by trapped flux from vertical (P_{mag_v}) and beam axis (P_{mag_b}) magnetic field for the Spiral2 QWR.

Table 2 summarizes and compares, for the three types of cavities, the measured sensitivities to the calculated sensitivities taking into account the geometrical effect. One can appreciate how the relative error between calculated and measured sensitivities is greatly reduced.

Table 2: Corrected Sensitivities (nΩ/mG)

Type of cavity	Measured component	Calculated-sensitivity	Measured sensitivity (error)
QWR	Vertical	0.011	0.006 (-45%)
QWR	Beam axis	0.048	0.05 (+4%)
SSR	Vertical	0.047	0.043 (-8.5%)
DSR	Beam axis	0.055	0.06 (+9%)

CONCLUSION

Flux trapping measurements done at IPNO on several type of resonators (QWR, Spoke) are revealing very clearly a strong geometrical dependence of the sensitivity to magnetic flux trapping. The real sensitivity, evaluated indirectly and globally by RF power measurements, is consistently lower than the theoretical sensitivity regardless the quality and history of the Niobium material. Assuming that only the normal component of the residual magnetic field is trapped during the superconducting transition appears to be a reasonable hypothesis. A very good agreement between calculated and measured sensitivities is obtained when geometrical corrections are applied thanks to the model presented here. Moreover, a clear linear correlation is measured between the “zero field” surface resistance (R_0) and the field dependent resistance (R_1) and is significantly affected by surface and heat treatments. Even though R_1 is increasing with the amount of trapped flux, this linear dependence doesn’t seem to be caused directly by trapped flux as even temperature make it rise.

REFERENCES

[1] H. Padamsee, *RF superconductivity for accelerators*. John Wiley & Sons, INC, New York, USA, 1998.

[2] S. Candia *et al.*, “Angular dependence of the magnetization of isotropic superconductors: which is the vortex direction?”, *Supercond. Sci. Technol.*, vol. 12, pp 192-198, 1999.

[3] S. Posen *et al.*, “Efficient expulsion of magnetic flux in superconducting radiofrequency cavities for high Q0 applications”, *J. Appl. Phys*. vol. 119, p. 213903, 2016.

[4] A. Romanenko *et al.*, “Ultra-high quality factors in superconducting niobium cavities in ambient magnetic fields up to 190 mG”, *Appl. Phys. Lett.* , vol. 105, p. 234103, 2014.

[5] C. Marchand *et al.*, “Performances of Spiral2 Low and High Beta Cryomodules”, in *Proc. SRF'15*, Whistler, Canada, Sep. 2015, paper WEBA04, pp. 967-972.

[6] P. Duchesne *et al.*, “Design of the 352 MHz, Beta 0.50, Double-Spoke Cavity for ESS”, in *Proc. SRF'13*, Paris, France, Sep. 2013, paper FRIOC01, pp. 1212-1217.

[7] D. Longuevergne *et al.*, “Performances of the two first single spoke prototypes for the MYRRHA project”, in *Proc. LINAC'16*, East Lansing, MI, USA, Sep. 2016, pp. 916-919. doi:10.18429/JACoW-LINAC2016-THPLR030

[8] Bartington, https://www.bartington.com/

[9] D. Longuevergne *et al.*, “Surface resistance study on low frequency (low beta) cavities”, in *Proc. SRF'15*, Whistler, Canada, Sep. 2015, paper WEA1A02.

[10] S. Aull *et al.*, “Trapped magnetic flux in superconducting niobium samples”, *Phys. Rev. Accel. Beams*, vol. 15, p. 062001, 2012.

[11] J. Halbritter *et al.*, “Additional losses in high purity niobium cavities related to slow cooldown and hydrogen segregation”, in *Proc. of the Sixth Workshop on RF Superconductivity, CEBAF, Newport News, Virginia, USA*, 1993.

[12] CST Microwave Studio, https://www.cst.com/products/cstmws